15 February 2002

ELSEVIER

Optics Communications 202 (2002) 311–318

OPTICS COMMUNICATIONS

www.elsevier.com/locate/optcom

Effects of carrier transport on the transverse-mode selection of index-guided vertical-cavity surface-emitting lasers

M.S. Torre[a], C. Masoller[b,*]

[a] *Instituto de Fìsica "Arroyo Seco", U.N.C.P.B.A Pinto 399 (7000) Tandil, Argentina*
[b] *Instituto de Fìsica, Facultad de Ciencias, Universidad de la República, Igua 4225, Montevideo 11400, Uruguay*

Received 15 August 2001; received in revised form 19 November 2001

Abstract

We study the transverse mode selection of a weakly index-guided vertical-cavity surface-emitting laser (VCSEL), based on an extension of the model of Valle et al. [Opt. Commun. 115 (1995) 297]. In the model we incorporate carrier capture and escape processes between the separate confinement heterostructure (SCH) layer and the quantum well (QW) active region of a VCSEL. These effects are characterized with phenomenological capture and escape times, τ_{cap}, τ_{esc}. We show analytically and by numerical simulations that when the carrier loss in the SCH region is taken into account, carrier capture and escape critically affects the transverse-mode selection of a VCSEL. A large ratio between τ_{cap} and τ_{esc} diminishes the number of photons in the QWs, leading to a decrease of the spatial-hole burning, which in turn benefits emission on the fundamental transverse mode. On the contrary, a small ratio between τ_{cap} and τ_{esc} increases the number of photons in the QWs, leading to a large spatial-hole burning which in turn favors higher-order transverse modes. If the carrier loss in the SCH region is neglected the total number of photons in the QW region is independent of τ_{cap} and τ_{esc}. In this case carrier capture and escape play no fundamental role in the transverse-mode selection of the VCSEL, but modify the transient dynamics of the relaxation oscillations.

PACS: 42.55.Px; 42.60.Mi; 42.60.FC

Keywords: Vertical-cavity surface-emitting lasers; Quantum-well lasers; Carrier dynamics; Carrier transport; Transverse-mode behavior

1. Introduction

The vertical-cavity surface-emitting laser (VCSEL) is a type of laser that is emerging as a key element for high-speed information processing systems and communication networks [1]. The advantages of a VCSEL over a conventional, edge-emitting semiconductor laser are single longitudinal mode operation, dense packing capability, low threshold current, high modulation bandwidth, narrow circular beam profile, and that it can be simply and efficiently coupled to an optical fiber. Near threshold operation VCSELs typically emit linearly polarized light in the fundamental transverse mode. However, it is often observed that the

* Corresponding author. Tel.: +598-2-5258618/307; fax: +598-2-5250580.
E-mail address: cris@fisica.edu.uy (C. Masoller).

0030-4018/02/$ - see front matter
PII: S0030-4018(01)01734-5

polarization state selected at threshold becomes unstable as the injection current is increased, and a switch to the orthogonal polarization state occurs [2]. For high power operation, high-order transverse modes are excited and the VCSEL usually emits multiple modes [3]. The complex polarization and transverse-mode dynamics of VCSELs are considered negative properties from the point of view of most applications and have received considerable attention (see, e.g., [4] and references therein).

It has been shown that carrier transport effects, i.e., carrier capture into and escape out of the quantum well (QW) region, and carrier diffusion across the separate confinement heterostructure (SCH) region, significantly degrade the modulation response of QW lasers [5–13]. The carrier capture and escape phenomena involve transitions between the three-dimensional SCH layer states and the two-dimensional QW states. These processes are usually modeled based on the 'reservoir' model [5–7]. The model considers two carrier densities, one associated with the carriers in the QW region, and one associated with the carriers in the SCH region. Carrier capture and escape are characterized by small but finite capture and escape times. The very fast capture time ($\sim$1–50 ps) can be considered too small to be of importance in the dynamics of VCSELs, even under high-speed modulation. However, the model predicts that the effect of a large ratio between capture and escape times on the modulation response is equivalent to the effect of a relatively large gain compression factor [6,7].

In this paper we study the effect of carrier transport on the transverse mode selection of a VCSEL. Since we focus on carrier transport effects, we consider a relatively simple model for a VCSEL, where polarization, temperature, and noise are effects not taken into account. Our model is an extension of the model proposed by Valle et al. [14,15] for a weakly index guided VCSEL (for which the transverse modes are determined by the waveguide structure). The model proposed by Valle et al. considers explicitly transverse profiles for the optical modes, and for the carrier density in the active region. The model was extended in [16,17] to consider the polarization degree of freedom, allowing the study of polarization and transverse effects in birefringent index-guided VCSELs. Here we extend the model of [14,15] with an equation for the carriers in the SCH region, following the approach of the 'reservoir' model [5–7]. Our model therefore combines two well-known models and allows the study of the interplay of transverse and carrier transport effects.

We find that the ratio between the capture and escape times strongly influences the transverse-mode selection of the VCSEL when the carrier loss in the SCH region is taken into account. On the contrary, if the carrier loss in the SCH region is neglected, capture and escape times play no significant role in the transverse-mode selection. However, in this case the finite capture time plays a role that is similar to the gain saturation parameter that is often included to model phenomenologically carrier transport among other effects (as spectral hole burning, carrier heating, etc.). This is in agreement with the results of [6,7].

This paper is organized as follows. Section 2 describes the extension of the model of Valle et al. [14,15] to include carrier capture and escape phenomena. In Section 3 we study the stationary solutions of the model, and their dependence on the carrier capture and escape times. Section 4 presents the results of numerical simulations, and Section 5 presents a summary and the conclusions.

2. Model

We consider a cylindrical weakly index guided VCSEL for which the appropriate transverse modes are the LP_{mn} modes. Polar coordinates (r,ϕ) are used to write the equations for the intensity of the LP_{mn} mode, $I_{mn}(t)$, the carrier density in the QW region, $n_w(r,\phi,t)$, and the carrier density in the SCH region, $n_b(r,\phi,t)$ [5–7,14,15]:

$$\frac{\mathrm{d}I_{mn}(t)}{\mathrm{d}t} = \left(g_{mn} - \frac{1}{\tau_{pmn}}\right) I_{mn}, \tag{1}$$

$$\frac{\partial n_b(r,\phi,t)}{\partial t} = \frac{j}{ed_b} - \frac{n_b}{\tau_{\mathrm{cap}}} + \frac{V_{\mathrm{qw}}}{V_b}\frac{n_w}{\tau_{\mathrm{esc}}} - \frac{n_b}{\tau_b} + D_b\nabla^2 n_b, \tag{2}$$

$$\frac{\partial n_w(r,t)}{\partial t} = \frac{V_b}{V_{qw}}\frac{n_b}{\tau_{cap}} - \frac{n_w}{\tau_{esc}} - \frac{n_w}{\tau_w} - \sum g_0(n_w - n_t)I_{mn}|\psi_{mn}|^2 + D_w\nabla^2 n_w. \quad (3)$$

Throughout the calculations we assume that the carrier variables are averaged along the longitudinal axis. Therefore, $n_w(r,\phi,t)$ represents the average carrier density in the (r,ϕ) point of the transverse plane, in the QW region (if the QW region consists of several QWs, interwell carrier transport effects are not considered, and n_w represents the average carrier density in the QWs). $n_b(r,\phi,t)$ represents the average carrier density in the (r,ϕ) point of the transverse plane in the SCH region.

In Eqs. (1)–(3), the modal intensities are normalized such that $I_{mn}|\psi_{mn}|^2$ is the photon density in the LP_{mn} mode, and the mode profiles are normalized such that

$$\int_0^\infty \int_0^{2\pi} |\psi_{mn}(r,\phi)|^2 r\,dr\,d\phi = 1. \quad (4)$$

g_{mn} is the modal gain given by

$$g_{mn}(t) = \int_0^\infty \int_0^{2\pi} \Gamma_{mn} g_0(n_w - n_t)|\psi_{mn}|^2 r\,dr\,d\phi, \quad (5)$$

where g_0 is the gain coefficient, Γ_{mn} is the confinement factor for the LP_{mn} mode, and n_t is the transparency carrier density. τ_{pmn} is the photon lifetime for the LP_{mn} mode.

The terms in the right-hand side of (2) correspond, from left to right, to:

(i) the rate at which carriers are injected into the SCH region,
(ii) the rate at which carriers are captured into the QWs,
(iii) the rate at which carriers escape out of the QWs,
(iv) the carrier loss owing to various non-radiative recombination processes, and
(v) the last term accounts for carrier diffusion across the SCH region.

$j(r,\phi)$ is the injected current, e is the electron charge, d_b is the thickness of the SCH region, τ_{cap} is the capture time, τ_{esc} is the escape time, τ_b is the carrier lifetime, ∇^2 is the transverse Laplacian operator, and D_b is the diffusion coefficient. Since n_b and n_w refer to carrier densities, the different sizes of the SCH and QW regions must be taken into account. This is done by the ratio V_b/V_{qw}, where $V_b(V_{qw})$ is the volume of the SCH (QW) region.

The terms in the right-hand side of (3) correspond, from left to right, to:

(i) the carriers captured into the QWs,
(ii) the carriers that escape out of the QWs,
(iii) the non-radiative carrier loss, τ_w,
(iv) the carrier loss owing to stimulated recombination, and
(v) the final term to carrier diffusion across the QWs.

3. Stationary solutions

The stationary solutions of (1)–(3) can be written as

$$I_{mn}(t) = I^s_{mn},$$
$$n_w(r,\phi,t) = n^s_w(r,\phi),$$
$$n_b(r,\phi,t) = n^s_b(r,\phi),$$

where I^s_{mn}, $n^s_w(r,\phi)$, and $n^s_b(r,\phi)$ satisfy

$$g^s_{mn} = \int_0^\infty \int_0^{2\pi} \Gamma_{mn} g_0\left(n^s_w - n_t\right)|\psi_{mn}|^2 r\,dr\,d\phi = \frac{1}{\tau_{pmn}}, \quad (6)$$

$$n^s_b\left(\frac{1}{\tau_{cap}} + \frac{1}{\tau_b}\right) = \frac{j}{ed_b} + \frac{V_{qw}}{V_b}\frac{1}{\tau_{esc}} n^s_w + D_b\nabla^2 n^s_w, \quad (7)$$

$$n^s_w\left(\frac{1}{\tau_{esc}} + \frac{1}{\tau_w}\right) = \frac{V_b}{V_{qw}}\frac{1}{\tau_{cap}} n^s_b - \sum I^s_{mn} g_0\left(n^s_w - n_t\right)|\psi_{mn}|^2 + D_w\nabla^2 n^s_w. \quad (8)$$

Eq. (6) shows that the steady-state value of the modal gain does not depend on carrier capture and escape times. Integrating (7) and (8) on the transverse plane and using (6) gives

$$\begin{aligned}
&\left(\gamma_{\rm cap}+\gamma_b\right)\int_0^{\infty}\int_0^{2\pi} n_b^s r\,{\rm d}r\,{\rm d}\phi \\
&\quad=\frac{1}{ed_b}\int_0^{\infty}\int_0^{2\pi} jr\,{\rm d}r\,{\rm d}\phi \\
&\qquad+\frac{V_{\rm qw}}{V_b}\gamma_{\rm esc}\int_0^{\infty}\int_0^{2\pi} n_w^s r\,{\rm d}r\,{\rm d}\phi \\
&\qquad+D_b\int_0^{\infty}\int_0^{2\pi}\nabla^2 n_b^s r\,{\rm d}r\,{\rm d}\phi, \qquad (9)\\
&\left(\gamma_{\rm esc}+\gamma_w\right)\int_0^{\infty}\int_0^{2\pi} n_w^s r\,{\rm d}r\,{\rm d}\phi \\
&\quad=\frac{V_b}{V_{\rm qw}}\gamma_{\rm cap}\int_0^{\infty}\int_0^{2\pi} n_b^s r\,{\rm d}r\,{\rm d}\phi-\sum\gamma_{pmn}I_{mn}^s \\
&\qquad+D_w\int_0^{\infty}\int_0^{2\pi}\nabla^2 n_w^s r\,{\rm d}r\,{\rm d}\phi, \qquad (10)
\end{aligned}$$

where $\gamma_{\rm esc}=1/\tau_{\rm esc}$, $\gamma_{\rm cap}=1/\tau_{\rm cap}$, $\gamma_b=1/\tau_b$, $\gamma_w=1/\tau_w$ and $\gamma_{pmn}=1/\Gamma_{mn}\tau_{pmn}$. The integral of the transverse Laplacian gives

$$\begin{aligned}
&\int_0^{2\pi}\int_0^{\infty}\left[\frac{1}{r}\frac{\partial}{\partial r}\left(r\frac{\partial n_b^s}{\partial r}\right)+\frac{1}{r^2}\frac{\partial^2 n_b^s}{\partial\phi^2}\right]r\,{\rm d}r\,{\rm d}\phi \\
&\quad=\int_0^{2\pi}\left\{\int_0^{\infty}\left[\frac{\partial}{\partial r}\left(r\frac{\partial n_b^s}{\partial r}\right)\right]{\rm d}r\right\}{\rm d}\phi \\
&\qquad+\int_0^{\infty}\left\{\int_0^{2\pi}\left[\frac{1}{r}\frac{\partial^2 n_b^s}{\partial\phi^2}\right]{\rm d}\phi\right\}{\rm d}r \\
&\quad=\int_0^{2\pi} r\frac{\partial n_b^s}{\partial r}\bigg|_{r=0}^{r=\infty}{\rm d}\phi+\int_0^{\infty}\frac{1}{r}\frac{\partial n_b^s}{\partial\phi}\bigg|_{\phi=0}^{\phi=2\pi}{\rm d}r=0.
\end{aligned} \qquad (11)$$

Since the diffusion terms vanish, (9) and (10) can be simplified to

$$\left(\gamma_{\rm cap}+\gamma_b\right)N_b^s=J+\gamma_{\rm esc}N_w^s, \qquad (12)$$

$$\left(\gamma_{\rm esc}+\gamma_w\right)N_w^s=\gamma_{\rm cap}N_b^s-\sum\gamma_{pmn}I_{mn}, \qquad (13)$$

where

$$N_b^s=d_b\int_0^{\infty}\int_0^{2\pi} n_b^s r\,{\rm d}r\,{\rm d}\phi,$$

$$N_w^s=d_{\rm qw}\int_0^{\infty}\int_0^{2\pi} n_w^s r\,{\rm d}r\,{\rm d}\phi$$

are the steady-state number of carriers in the SCH and QW regions, respectively. Here $d_{\rm qw}$ is the thickness of the QW region, and

$$J=\frac{1}{e}\int_0^{\infty}\int_0^{2\pi} jr\,{\rm d}r\,{\rm d}\phi$$

is the number of injected carriers per unit time.

The non-radiative recombination time in the SCH region τ_b determines whether carrier capture and escape have a relevant effect on the dynamics or not.

First, we consider the case when the recombination times in the SCH and QW regions are equal: $\gamma_b=\gamma_w=\gamma_n$. In this case we can eliminate N_b^s from (12) and (13) and obtain

$$\begin{aligned}
\sum\gamma_{pmn}I_{mn}=&\frac{J}{1+\gamma_n/\gamma_{\rm cap}}-\frac{\gamma_n N_w^s}{1+\gamma_n/\gamma_{\rm cap}} \\
&\times\left(1+\frac{\gamma_n}{\gamma_{\rm cap}}+\frac{\gamma_{\rm esc}}{\gamma_{\rm cap}}\right).
\end{aligned} \qquad (14)$$

Here, two limits are interesting to consider. When the carriers do not escape out of the QW region ($\gamma_{\rm esc}\approx 0$), we recover the simple connection between the photon number, the injected current, and the carrier number in the active region,

$$\sum\gamma_{pmn}I_{mn}=J_{\rm eff}-\gamma_n N_w^s \qquad (15)$$

with a modified, 'effective' injected current given by,

$$J_{\rm eff}=J\left(1+\gamma_n/\gamma_{\rm cap}\right)^{-1} \qquad (16)$$

which is slightly lower than the actual injected current (typically, τ_n is of the order of nanoseconds, and $\tau_{\rm cap}$ is of the order of picoseconds, thus $\gamma_n/\gamma_{\rm cap}\ll 1$). The factor $(1+\gamma_n/\gamma_{\rm cap})^{-1}$ represents the carriers lost (due to non-radiative processes), during the capture time. In other words, a finite capture time diminishes the current density effectively injected into the QWs.

The other limit corresponds to a fast escape of carriers out of the QW region ($R=\tau_{\rm cap}/\tau_{\rm esc}=\gamma_{\rm esc}/\gamma_{\rm cap}\gg 1$). This leads to a larger, negative contribution of the last term in (14), and therefore to a significant reduction of the total number of photons in the QW region. This leads in turn decreases the spatial hole burning, and thus, modifies which transverse modes have enough gain to operate above threshold.

Second, we consider the case when the non-radiative carrier loss in the SCH region is negligible, $\gamma_b = 0$. In this case we can eliminate N_b^s from (12) and (13) and obtain

$$\sum \gamma_{pmn} I_{mn} = J - \gamma_w N_w^s. \tag{17}$$

In (17) carrier capture and escape plays no role on the steady-state value of the total intensity, and therefore, it will not have a relevant role in the spatial-hole burning (it affects only the number of carriers in the SCH region). Since in the model the fact that determines if a mode operates above threshold is its overlap with the carrier profile, we expect that in this case R does not have a strong influence on the transverse mode selection (it might, however, have an effect on the transient dynamics).

A complementary way to understand the effect of carrier capture and escape is considering the dependence of the threshold current of the fundamental transverse mode on the capture and escape times. The threshold current can be estimated from (2) and (3) neglecting the diffusion terms. After some manipulation we obtain

$$\frac{j_{\rm th}}{ed_b} = \frac{V_{\rm qw}}{V_b}\left[\frac{\gamma_{\rm esc}\gamma_b + \gamma_w(\gamma_{\rm cap} + \gamma_b)}{\gamma_{\rm cap}}\right] n_w^{\rm th}, \tag{18}$$

where $n_w^{\rm th} = n_t + (\tau_{p01}\Gamma_{01}g_0)^{-1}$. Clearly, if $\gamma_b = 0$, $\gamma_{\rm cap}$ and $\gamma_{\rm esc}$ do not modify the threshold current. On the contrary, if $\gamma_b \neq 0$, an increase of $\gamma_{\rm esc}$ leads to an increase of the threshold current, and therefore, for a fixed injection current the laser operates closer to threshold.

4. Numerical results

Next, we show the results of numerical simulations that confirm the previous analysis. To simplify the calculations we consider that the injected current is azimuthally uniform over the active area, and consider three modes which are azimuthally symmetric: LP_{01}, LP_{11} and LP_{02} (LP_{11} is degenerate and its profile is azimuthally independent [18]). The equations were integrated with the laser parameters given in Table 1, a time integration step of $\Delta t = 0.1$ ps and a space integration step of $\Delta x = 0.02$ μm.

Fig. 1 shows the dynamics when the carrier loss in the SCH region is taken into account ($\tau_b = \tau_w = 1.52$ ns). We plot the laser turn-on, for the same injected current ($I = j\pi a^2 = 1.6$ mA) and four decreasing values of the escape time. For a large escape time (Fig. 1(a), $\tau_{\rm esc} = 0.5$ ns), the modes LP_{01}, and LP_{11} turn on. The total intensity (solid line) is large enough such that (due to spatial-hole burning), the mode LP_{11} (dot-dashed line) dominates over the fundamental mode LP_{01} (dashed line). For a lower escape time (Fig. 1(b), $\tau_{\rm esc} = 50$ ps), there is a larger delay on the laser turn-on, the total intensity is lower, and the modes LP_{01} (dashed line) and LP_{11} (dot-dashed line) have nearly equal power. If we continue to decrease the escape time, the intensity is very low and only the fundamental mode turns on (Fig. 1(c), $\tau_{\rm esc} = 30$ ps, notice the different vertical scales). For even lower escape time (Fig. 1(d), $\tau_{\rm esc} = 5$ ps), the carriers do not stay in the QW region long enough to provide gain, and the laser does not turn-on.

Table 1
Parameters involved in Eqs. (1)–(3) and typical values used in the numerical simulations

Radius of the transverse area	a	6 μm
Thickness of the QW region	$d_{\rm qw}$	0.024 μm (three QWs of thickness 0.08 μm)
Thickness of the SCH region	d_b	1.2 μm
Group velocity	v_g	7.147×10^4 μm/ns
Differential gain	$\partial g/\partial n$	5.946×10^{-8} μm^2
Gain coefficient	$g_0 = v_g \partial g/\partial n$	4.25×10^{-3} μm^3/ns
Confinement factor (same for all modes)	Γ	0.0382
Carrier density at transparency	n_t	1.33×10^6 μm^{-3}
Linewidth enhancement factor	α	3
Photon lifetime (same for all modes)	τ_p	2.2 ps
Injection current	$I = j\pi a^2$	1.6 mA
Diffusion coefficient	D_b, D_w	5 cm^2/s

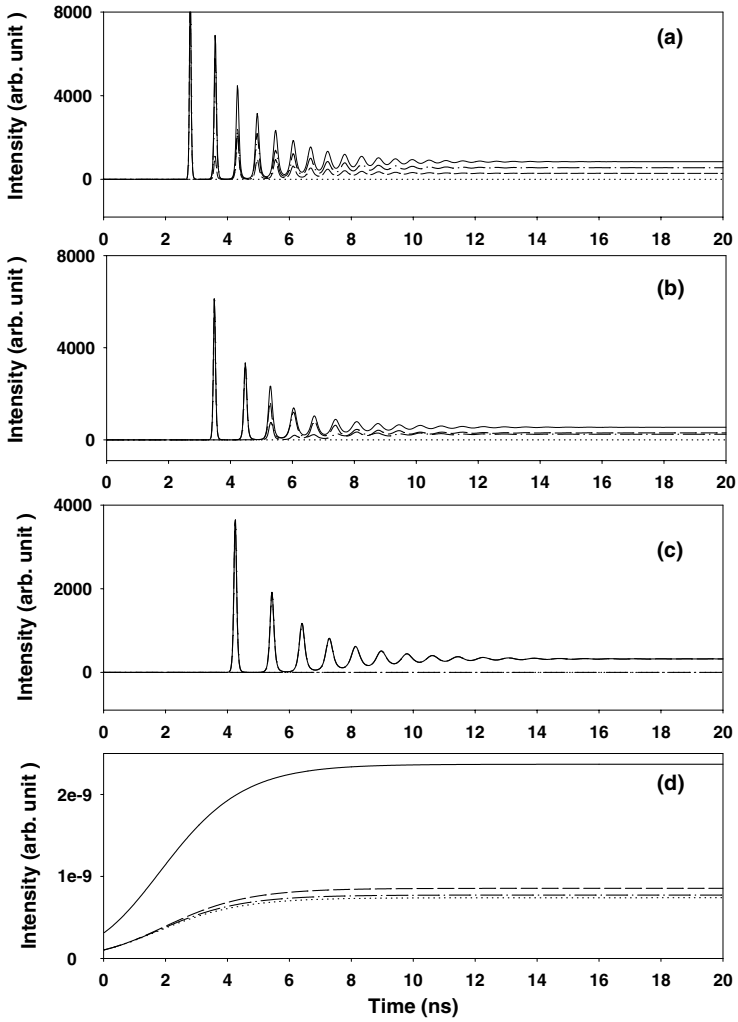

Fig. 1. Turn-on transient dynamics when $\tau_b = \tau_w = 1.52$ ns, $\tau_{cap} = 5$ ps: (a) $\tau_{esc} = 500$ ps; (b) $\tau_{esc} = 50$ ps; (c) $\tau_{esc} = 30$ ps; (d) $\tau_{esc} = 5$ ps. The solid line shows the total intensity, the dot-dashed line shows the LP_{11} modal intensity, the dotted line shows LP_{02} modal intensity and the dashed line shows the LP_{01} modal intensity. The injected current ($I = 1.6$ mA) is (a) $1.34I_{th}$ ($I_{th} = 1.19$ mA); (b) $1.23I_{th}$ ($I_{th} = 1.30$ mA); (c) $1.16I_{th}$ ($I_{th} = 1.38$ mA); (d) $0.68I_{th}$ ($I_{th} = 2.36$ mA).

The results shown in Fig. 1 are to be expected, since a large ratio $R = \tau_{cap}/\tau_{esc}$ implies a very inefficient laser with poor carrier confinement in the QW region. This effect can be quantitatively understood in two complementary ways, as explained previously. On the one hand, for non-zero spontaneous recombination in the SCH region, an increase of γ_{esc} increases the laser threshold current, favoring the fundamental mode emission. In the figure caption we give the values of effective threshold currents, which are slightly larger than the values calculated from Eq. (18), because Eq. (18) was obtained not taking into account carrier diffusion. On the other hand, an increase of γ_{esc} increases the last term in the RHS of Eq. (14), thus leading to a lower number of photons in the QWs, in turn favoring fundamental mode emission. We have verified that for the value of R as in Fig. 1(a), if we consider an injection current which is the same percentage above threshold as in Fig. 1(c)

(i.e., for $I = 1.16I_{th}$, where $I_{th} = 1.19$ mA is the threshold current when $\tau_{esc} = 0.5$ ns) we observe the same single-mode dynamics as in Fig. 1(c). In other words, the effect of decreasing τ_{esc} for a fixed injection current is the same as decreasing the injection current for a fixed τ_{esc}: in both cases the laser is closer to threshold and tends to operate on the fundamental transverse mode.

Fig. 2 shows the dynamics when the non-radiative carrier loss in the SCH region is negligible ($\gamma_b = 0$) and all other parameters as Fig. 1. In this case the escape time does not modify the value of the final total intensity. A decrease of the escape time affects the transient dynamics, reducing the frequency of the relaxation oscillations of the total intensity and increasing the transient relaxation time (notice that in Fig. 2(a) the oscillations are more damped than in Fig. 2(d), and the steady-state is reached sooner). These results agree well with the results of Nagarajan et al. [6], in spite of the fact that in [6] a simpler model was used (which was single-mode and did not consider transverse effects). Notice also that in Figs. 2(a)–(c) the LP_{11} mode dominates over the LP_{01} mode, while the opposite occurs in Fig. 2(d). This is due to the long delay in the laser turn-on, which leads to the initial turn-on of the fundamental mode. Later on the LP_{11} mode turns on (at about $t \sim 12$ ns), but is not

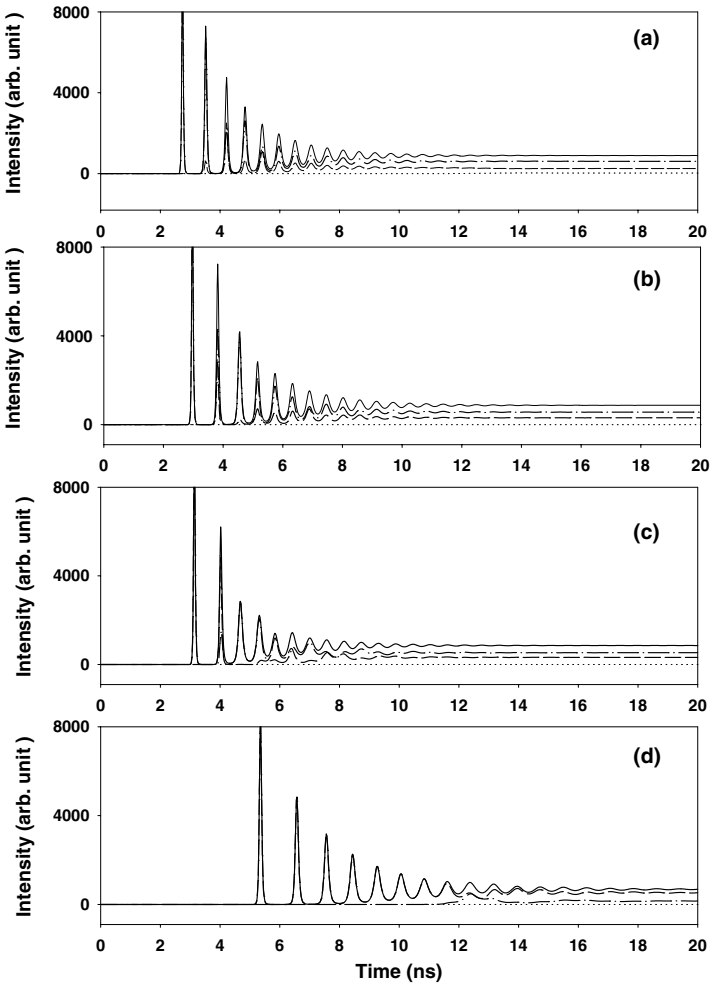

Fig. 2. Turn-on transient dynamics when $\gamma_b = 0$, all other parameters as Fig. 1. Here $I = 1.6$ mA $= 1.36I_{th}$ ($I_{th} = 1.18$ mA).

strong enough to gain carriers from the LP_{01} mode, which dominates. This effect of carrier capture and escape on the transverse mode partition of the total power is also a consequence of fact that carrier capture and escape modifies the transient relaxational dynamics.

5. Summary and conclusions

To summarize, we have studied the effect of carrier capture and escape on the dynamics of a weakly index-guided VCSEL, and have shown that when the non-radiative carrier loss in the SCH region is taken into account, the transverse mode selected depends strongly on the escape time out of the QWs. Fast carrier escape leads to a reduction of the total number of photons in the QW region and benefits operation on the fundamental transverse mode. On the contrary, for slow carrier escape the laser intensity is high, which leads to strong spatial-hole burning that induces the coexistence of two transverse modes. If the carrier loss in the SCH region is negligible carrier capture and escape has no effect on the total number of photons in the QW region, but strongly modifies the transient dynamics.

Since we have found that the effect of carrier transport when carrier loss in the SCH region is taken into account differs from when it is neglected, we speculate that differences would arise also on the modulation response, and on the transverse mode dynamics. It would also be of interest to consider a more realist model for the gain, that takes into account the carrier non-linear dependence. These studies are the objective of future work.

Acknowledgements

M.S. Torre is supported in part by a grant from Secretaría de Ciencia y Técnica (UNCPBA-Argentina), and C. Masoller is supported in part by PEDECIBA and CSIC (Uruguay).

References

[1] K.D. Choquette, D.G. Deppe (Eds.), Vertical-Cavity Surface-Emitting Lasers, SPIE Proc., 3003, SPIE, Bellingham, 1997.
[2] K.D. Choquette, K.L. Lear, R.E. Leibenguth, M.T. Asom, Appl. Phys. Lett. 64 (1994) 2767.
[3] C.J. Chang-Hasnain, M. Orenstein, A. Von Lehmen, L.T. Florez, J.P. Harbison, N.G. Stoffel, Appl. Phys. Lett. 57 (1990) 218.
[4] M. San Miguel, Polarization properties of VCSELs, in: A. Miller (Ed.), Semiconductor Quantum Optoelectronics, Institute of Physics, 1999.
[5] W. Rideout, W.F. Sharfin, E.S. Koteles, M.O. Vassell, B. Elman, IEEE Photon. Technol. Lett. 3 (1991) 784.
[6] R. Nagarajan, T. Fukushima, S.W. Corzine, J.E. Bowers, Appl. Phys. Lett. 59 (1991) 1835.
[7] R. Nagarajan, M. Ishikawa, T. Fukushima, R.S. Geels, J.E. Bowers, IEEE Photon. Technol. Lett. 4 (1992) 121.
[8] S.C. Kan, D. Vassilovski, T.C. Wu, K.Y. Lau, Appl. Phys. Lett. 61 (1992) 752.
[9] K.Y. Lau, in: P.S. Zory Jr. (Ed.), Quantum Well Lasers, Academic, San Diego, 1993, p. 217.
[10] A.G. Plyavenek, Opt. Commun. 113 (1994) 259.
[11] C.Y. Tsai, Y.H. Lo, R.M. Spencer, Appl. Phys. Lett. 67 (1995) 3084.
[12] M. Kucharczyk, M.S. Wartak, P. Weetman, IEEE Photon. Technol. Lett. 11 (1999) 1226.
[13] M.S. Torre, H.F. Ranea-Sandoval, IEEE J. Quantum Electron. 36 (2000) 112.
[14] A. Valle, J. Sarma, K.A. Shore, Opt. Commun. 115 (1995) 297.
[15] A. Valle, J. Sarma, K.A. Shore, IEEE J. Quantum Electron. 31 (1995) 1423.
[16] J. Martin-Regalado, S. Balle, M. San Miguel, A. Valle, L. Pesquera, Quantum Semiclass. Opt. 9 (1997) 713.
[17] A. Valle, J. Martin-Regalado, L. Pesquera, S. Balle, M. San Miguel, in: Physics and Simulation of Optoelectronic Devices, vol. VI, SPIE, Bellingham, Washington, 1998, p. 280, Paper 3283-32.
[18] J. Dellunde, A. Valle, L. Pesquera, K.A. Shore, J. Opt. Soc. Am. B 16 (1999) 2131.